# Characterization and functional analyses of novel chicken leukocyte immunoglobulin-like receptor subfamily B members 4 and 5

Anh Duc Truong,[*,†] Yeojin Hong,[*] Ha Thi Thanh Tran,[†] Hoang Vu Dang,[†] Viet Khong Nguyen,[†] Thu Thao Pham,[*] Hyun S. Lillehoj,[‡] and Yeong Ho Hong[*,1]

[*]*Department of Animal Science and Technology, Chung-Ang University, Anseong 17546, Republic of Korea;* [†]*Department of Biochemistry and Immunology, National Institute of Veterinary Research, 86 Truong Chinh, Dong Da, Hanoi 100000, Viet Nam; and* [‡]*Animal Biosciences and Biotechnology Laboratory, Agricultural Research Services, United States Department of Agriculture, Beltsville, MD 20705, USA*

**ABSTRACT** The inhibitory leukocyte immunoglobulin-like receptors (**LILRBs**) play an important role in innate immunity. Currently, no data exist regarding the role of LILRB4 and LILRB5 in the activation of immune signaling pathways in mammalian and avian species. Here, we report for the first time, the cloning and structural and functional analyses of chicken LILRB4–5 genes identified from 2 genetically disparate chicken lines. Comparison of LILRB4–5 amino acid sequences from lines 6.3 and 7.2 with those of mammalian proteins revealed 17 to 62% and 19 to 29% similarity, respectively. Phylogenetic analysis indicated that the chicken LILRB4–5 genes were closely associated with those of other species. LILRB4–5 could be subdivided into 2 groups having distinct immunoreceptor tyrosine-based inhibitory motifs, which bind to Src homology 2-containing tyrosine phosphatase 2 (**SHP-2**). Importantly, LILRB4–5 also upregulated the major histocompatibility complex (**MHC**) class I and $\beta$2-microglobulin gene expression as well as the expression of transporter associated with antigen processing 1–2, which play an important role in MHC class I activation. Our results indicate that LILRB4–5 are transcriptional regulators of the MHC class I pathway components and regulate innate immune responses. Furthermore, LILRB4–5 could activate the Janus kinase/signal transducer and activator of transcription (**JAK/STAT**) signaling pathway genes in macrophages and induce the expression of chemokines and T helper (**Th**)1, Th2, and Th17 cytokines. Our data suggest that LILRB4–5 are innate immune receptors associated with SHP-2, MHC class I, and $\beta$2-microglobulin. Additionally, they activate the JAK/STAT signaling pathway and control the expression of cytokines in macrophages.

**Key words:** cytokine, LILRB, MHC class I, signaling pathway

## INTRODUCTION

In mammals, leukocyte immunoglobulin (**Ig**)-like receptor subfamily B members (**LILRB**) are an inhibitory group comprising 5 functional genes, namely LILRB1 to LILRB5, also called ILT2/LIR-1/CD85j, ILT4/LIR-2/CD85D, ILT5/LIR-3/CD85a, ILT3/LIR-5/CD85k, and LIR-8/CD85c, respectively (Zhang et al., 2015a). These proteins are highly homologous in their extracellular regions (Kang et al., 2015; Zhang et al., 2015b). LILRBs are type I transmembrane glycoproteins, expressed predominantly on monocytes, macrophages, dendritic cells, B cells, natural killer cells, T cells, and granulocytes, thus demonstrating that LILRBs have a key role in immune cell functions (Zhang et al., 2015a). Recently, it was identified that LILRB4–5 interact with human leukocyte antigen (**HLA**) class I molecules and non-HLA ligands, and also induce the expression of cytokines (Kang et al., 2015; Zhang et al., 2015a; Zhang et al., 2015b). LILRB4 and LILRB5 belong to the group I of LILRBs and the structure of LILRB4–5 contains a signal peptide, Ig domains, transmembrane, cytoplasmic domain, and 2–3 immunoreceptor tyrosine-based inhibitory (**ITIM**) motifs (Kang et al., 2015; Zhang et al., 2015a). These ITIM motifs [(-I/V/L/S)xYxx(L/V-)] are located in the cytoplasmic tail and are responsible for the inhibitory signals transmitted by LILRBs (Burshtyn et al., 1997; Vivier and Daeron, 1997). ITIM motif is activated and induced by several phosphatases, including protein tyrosine phosphatase, non-receptor type 6 (**SHP-1**), SHP-2, or Src homology 2 domain-containing inositol phosphatase (**SHIP**) (Kang et al., 2015), resulting in the induction of various cytokines (Kang et al., 2015; Zhang et al., 2015a; Zhang et al., 2015b). Moreover, LILRB4–5 has been shown to regulate the Toll-like receptor signaling pathway, antigen-presentation, and cytokine production

(Brown et al., 2009), thus demonstrating that LILRB4–5 play an important role in the regulation of innate immune responses. Although LILRB4–5 have been associated with multiple diseases ranging from viral infection to autoimmunity, including *Salmonella* infection (Brown et al., 2009), rheumatoid arthritis (Tedla et al., 2011), Alzheimer's disease (Kim et al., 2013), psoriatic arthritis (Bergamini et al., 2014), HIV/AIDS (Bashirova et al., 2014), cancer (Zhang et al., 2015a), cytomegalovirus (Rothe et al., 2016), and *Mycobacterium tuberculosis* (Hogan et al., 2016), the mechanism underlying LILRB4–5-mediated activation and induction of cytokine expression has not been investigated.

In chicken, using bioinformatics approaches, Ig superfamily homolog genes such as TREM, CD300, SIRP, and chicken Ig-like receptors (**CHIR**)-A, CHIR-B, and CHIR-AB were identified to be involved in immune responses (Jansen et al., 2016). Recently, the expression of chicken leukocyte immunoglobulin receptor (**LIR**) family genes was evaluated, revealing a highly polymorphic locus harboring a variable number of CHIR genes, which also play an important role against avian influenza (Jansen et al., 2016). Moreover, in our previous study, we identified and characterized the chicken LILRA2, LILRA6, and LILRB1–3 genes. We demonstrated that these genes regulate the expression of the major histocompatibility complex (**MHC**) class I molecule, $\beta$2m, and cytokines through signaling pathways (Truong et al., 2018a; Truong et al., 2018b). However, pertinent information, such as the primary structure of LILRB4 and LILRB5 and their functions, is lacking in chicken.

Thus, in this study, we identified and characterized novel LILRB4 and LILRB5 gene variants in chicken, namely LILRB4R, -B4S, -B5R, and -B5S, which were isolated from two genetically disparate chicken lines.

## MATERIALS AND METHODS

### Antibodies

Mouse monoclonal GFPuv/eGFP antibody was purchased from R&D Systems (Minneapolis, MN, USA). The following reagents were from the indicated manufacturers: mouse anti-chicken MHC Class I-PE and mouse anti-chicken $\beta$2m-PE antibody (Southern Biotech, Birmingham, AL, USA); rabbit anti-chicken STAT1 (phospho-Ser[727]), anti-chicken STAT3 (phospho-Ser[727]), and anti-chicken JAK2 (phospho-Tyr[1007]/Tyr[1008]) antibody (Santa Cruz Biotech Dallas, Texas, USA); rabbit anti-chicken SOCS1, anti-chicken STAT1, anti-chicken STAT3 antibodies, horseradish peroxidase (**HRP**)-linked anti-rabbit secondary antibodies, and protein G–sepharose bead (Sigma-Aldrich, Louis, MO, USA); rabbit anti-chicken SHP2 (phospho-Tyr[542]), anti-chicken JAK2, and anti-chicken TYK2 antibody (Biorbyt, San Francisco, CA, USA); rabbit anti-chicken GAPDH antibody (Abcam, Cambridge,

MA, USA); Alexa Fluor® 488 Goat anti-rabbit IgG (H+L) secondary antibody (Invitrogen, Carlsbad, CA, USA); mouse monoclonal anti-chicken IFN-$\gamma$, IL-17A, IL-12p40 antibody and recombinants of these proteins (kindly provided by Dr. Hyun S. Lillehoj, USDA). EZ-LinkTM Sulfo-NHS-LC-Biotin, goat anti-mouse IgG secondary antibody linked HRP conjugate, and HRP-conjugated streptavidin were purchased from Thermo Scientific (Waltham, MA, USA).

### Identification of Chicken LILRB4-5 Genes by Bioinformatics

In our previous study, we identified approximately 15,000 novel transcripts that were differentially expressed in two chicken lines, namely resistant line 6.3 and susceptible line 7.2, which share the same MHC haplotype and show different levels of necrotic enteritis (**NE**) susceptibility (Truong et al., 2015a; Truong et al., 2015b). These sequences were used to search all current chicken genome assemblies through the *Gallus_gallus-5.0 reference Annotation Release 103* by BLAST program (https://blast.ncbi.nlm.nih.gov/Blast.cgi). The chromosomal locations were clarified using the BLAST-Like Alignment Tool (https://genome.ucsc.edu/FAQ/FAQblat.html) (Table S1). The genomic DNA identified as encoding potential chicken LILRB4–5 genes was then analyzed using GeneScan (http://genes.mit.edu/GENSCAN.html). Protein identification was conducted using the Expert Protein Analysis System (ExPASy; http://www.expasy.org/tools/). Multiple sequence alignments were analyzed using the Lasergene software (DNASTAR Inc. Madison, WI, USA). Phylogenetic analysis of LILRB4–5 amino acid sequences was conducted using the neighbor-joining method with a bootstrap value of 1,000 by the MEGA6 program. Signal peptides were predicted by SignalP 4.1 Server v.4.1 (www.cbs.dtu.dk/services/SignalP/). Glycosylation motifs were predicted using NetOGlyc 4.0 Server (www.cbs.dtu.dk/services/NetOGlyc/). The Ig domains, a transmembrane domain, and cytoplasmic regions were predicted by InterPro v.56.0 (http://www.ebi.ac.uk/interpro/). The ITIMs were mapped to each sequence, using the established V/L/S/NxYxxL/V ITIM motifs (Burshtyn et al., 1997; Vivier and Daeron, 1997). The structure and candidate ligand-biding site of proteins was predicted by molecular replacement using the RaptorX web server (raptorx.uchicago.edu/). To identify the function, the ligand of LILRB4–5 was mapped and searched in the RCSB protein data bank (http://www.rcsb.org) and from publications.

### Vector Construction and Cell Transfection

To clone full-length chicken LILRB4–5, the predicted LILRB4–5 coding sequences (**CDS**) from 2 chicken lines were amplified from total RNA isolated from chicken intestinal tissue. To verify the sequences, primers were

designed using the Lasergene software (DNASTAR Inc. Madison, WI, USA) and synthesized by Genotech Co. Ltd. (Daejeon, South Korea) (Table S2). The PCR products from 10 individual samples of the chicken line 6.3 or line 7.2 were purified using the QIAQuick Gel Extraction Kit (QIAgen, Hilden, Germany), and cloned into the pCR2.1-TOPO vector (Invitrogen) as previously described (Truong et al., 2016a; Truong et al., 2016b). Full-length CDS of LILRB4–5 genes were excised from pCR2.1 using *Not*I/*Xba*I (Bioneer Corp, Daejeon, South Korea) and ligated into the eukaryotic expression vector pcDNA3-eGFP (Addgene, Cambridge, MA, USA), followed by transformation into *E. coli* BL21 (Invitrogen); the positive clones were sequenced at Genotech. The plasmids were extracted, and endotoxins were removed using the PureYield Plasmid Midiprep System (Promega, Madison, WI, USA) as per manufacturer's instructions. The pcDNA3-eGFP vector containing the CDS of LILRB4R, -B4S, -B5R, or -B5S was transfected into chicken HD11 cells (Klasing and Peng, 1987) using Lipofectamine 3000 transfection reagent (Invitrogen), following the manufacturer's protocol. A mock transfection was also performed using the empty pcDNA3-eGFP vector. A total of $1.0 \times 10^6$ cells/well in 6-well plates were transfected with 4 μg of the plasmid and after 48 h, transfected cells were immediately transferred on ice, and subsequently pelleted by centrifugation for further analysis

## Flow Cytometry

Cells ($1.0 \times 10^6$) were re-suspended in staining buffer (10% FBS, 15 mM HEPES, and 2 mM EDTA in PBS) and primary antibodies were added, followed by incubation for 30 min on ice. To assess the expression of LILRA4–5-eGFP binding with MHC class I and $\beta$2m, anti-MHC class I-PE and anti-$\beta$2m-PE antibodies were applied, followed by a single wash with staining buffer. Next, to investigate how LILRA4–5-eGFP activates and regulates SHP-2, the anti-chicken SHP-2 antibody was added and incubated for 30 min on ice, followed by addition of Alexa Fluor 488-conjugated anti-rabbit secondary antibody (Invitrogen) and incubation for 30 min on ice. Control sections were treated with goat anti-chicken IgG-PE or rabbit IgG only (data not shown). Analysis by flow cytometry was performed with a BD FACSAria II cell sorter (BD Biosciences). Data were acquired using BD FACSDiva Version 6.1.3 and analyzed using FlowJo 7.6.1 software.

## Immunoprecipitation and Western Blotting

Cells were washed twice with ice-cold PBS and harvested in ice-cold RIPA buffer [50 mM Tris-HCl pH 7.5, 150 mM NaCl, 2 mM EDTA, 100 mM NaF, 0.1% SDS, 0.5% sodium deoxycholate, 1% Triton X-100, 10 mM $Na_4P_2O_7$, 10 mM $Na_3VO_4$] with complete EDTA-free protease inhibitor cocktail (Thermo Scientific). Cells were gently lysed for 30 min at 4°C and centrifuged at 13,000 *g* for 15 min at 4°C. Protein concentration

was determined using the Coomassie (Bradford) protein assay kit (Thermo Scientific) in microplates as per the manufacturer's instructions. Approximately, 100 μg protein was incubated with anti-eGFP mAb or anti-GAPDH antibody at 4°C overnight and then with 50 μL of Protein G–sepharose (Invitrogen) for 2 h. The immunoprecipitates were then washed three times in RIPA buffer and solubilized in 2 × SDS-PAGE sample buffer and heated to 100°C for 5 min. Samples were electrophoresed on 12% Tris-glycine SDS-PAGE gels, and protein transferred to PVDF membrane (GE Healthcare, Rydalmere, Australia). Membranes were blocked with 5% skim milk (Thermo Scientific) or 3% BSA (Sigma-Aldrich) in phosphate buffered saline (PBS) pH 7.4 containing 0.05% Tween 20 (**PBST**). Membranes were washed with PBST and incubated with anti-MHC class I, anti-$\beta$2m, anti-SHP-2 antibody, or signaling antibodies and incubated with the relevant secondary antibody in 2% skim milk or 0.5% BSA in PBST. Membranes were developed using Western Lightning ECL Plus (Thermo Scientific) and Hyperfilm (GE Healthcare).

## Enzyme-linked Immunosorbent Assay

A 96-well plate (Nunc Maxisorb, Nunc, Wiesbaden, Germany) was incubated with 1:500 dilutions of monoclonal anti-IFN-$\gamma$, IL-17A, or IL-12p40 antibody for 7 d at 4°C, as previously described (Truong et al., 2017). After blocking with 5% skim milk for 1 h at room temperature, the plate was incubated with culture supernatants of transfected cells or different dilutions of recombinant IFN-$\gamma$, IL-12p40, or IL-17A, overnight at 4°C. Following incubation with biotinylated-IFN-$\gamma$, -IL-12p40, or -IL-17A antibodies, HRP-conjugated streptavidin was added and incubated for 2 h at room temperature. The substrate $3,3',5,5'$-tetramethylbenzidine (TMB, Thermo Scientific) was used as a chemiluminescent substrate and luminescence was measured in a Hybrid Microplate Reader (Epoch, BioTek Instruments, Winooski, VT, USA).

## Real-time Quantitative PCR

After transfection for 48 h with a pcDNA3-eGFP vector containing the CDS of LILRB4R, -B4S, -B5R, -B5S, and mock control, cells were washed with ice-cold PBS and total RNA was extracted using TRIzol (Invitrogen). RNA was diluted with 20 μL of RNase-free $H_2O$ and the concentration was determined using the Hybrid Microplate Reader. For cDNA synthesis, up to 2 μg of RNA was treated with 1.0 unit of DNase I and 1 μL of 10 × reaction buffer (Thermo Scientific), and incubated for 30 min at 37°C. Subsequently, 1 μL of 50 mM EDTA was added and the samples were heated to 65°C for 10 min to inactivate the DNase I, followed by reverse transcription using the Maxima First Strand cDNA Synthesis Kit (Thermo Scientific), according to the manufacturer's recommendations. To analyze the expression of cytokines, we designed primers using

Lasergene software (Table S2) and performed qRT-PCR using 2 × Power SYBR Green Master Mix (Roche, Indianapolis, IN, USA), with the LightCycler 96 system (Roche). Chicken glyceraldehyde-3-phosphate dehydrogenase gene (**GAPDH**) was used as an internal control to normalize cytokine expression. The relative quantification of gene-specific expression was calculated using the $2^{-\Delta\Delta Ct}$ method after normalization to *GAPDH* (Livak and Schmittgen, 2001). All qRT-PCR was performed in triplicate.

## Cytotoxicity Test

To determine the cytotoxicity of LILRB4R, -B4S, -B5R, and -B5S linked pcDNA3-eGFP vectors and empty vector transfected into HD11 cells, after 48 h, cell proliferation and nitric oxide (**NO**) production assays were performed in 96-well plates according to well-established protocols (Truong et al., 2017). The nitrite content and cell proliferation were measured using the Griess reagent (Sigma-Aldrich) and Cell Counting Kit-8 (Dojindo Molecular Technologies, Inc., Mashikimachi, Kumamoto, Japan), respectively. Lipofectamine 3000 reagent and DMEM medium were used as controls.

## Statistical Analysis

Data are represented as the mean ± SEM of at least three independent experiments for each group ($n = 3$) and were analyzed with the SAS® 9.4 statistical program (SAS Institute Inc. Cary, NC, USA). Comparison between experimental groups was carried out using the Duncan's multiple method. Differences were considered significant for $P < 0.05$.

# RESULTS

## Identification of Potential LILRB4-5 Genes in 2 Genetically Dissimilar Chicken Lines

Based on our datasets from the 2 NE-induced genetically disparate chicken lines (Truong et al., 2015a; Truong et al., 2015b), we identified a total of 9 open reading frames (**ORFs**) in our library as containing potential chicken LILRB4 and LILRB5. The 9 ORFs were located on chromosome Un-random from the 999,034 to 63,829,571 position. Of the 9 ORF sequences, we considered 4 ORFs that contained Ig domains and differences between the two chicken lines for further analysis. Next, we evaluated the level of LILRB4R, -B4S, -B5R, and -B5S transcript expression in the two NE-induced chicken lines. The expression of LILRB4 and LILRB5 transcript in line 6.3 was higher than that in line 7.2 and higher under NE conditions than in controls (Tables S1). The novel mRNA transcripts of LILRB4R, -B4S, -B5R, and -B5S were detected by RT-PCR, cloned, and 10 individual samples from each chicken line were sequenced. Comparisons of nucleotide and amino acid sequence showed that LILRB4 and LILRB5 in the 10 samples of one chicken line were 100% identical (data not shown). Analysis of the LILRB4R, -B4S, -B5R, and -B5S nucleotide sequences showed similarities ranging from 25 to 41% with mammalian orthologs (data not shown). Multiple alignment of the predicted protein sequences of LILRB4 and LILRB5 in line 6.3 to those in line 7.2 showed 95 to 97% and 98 to 99% similarity, respectively (Table 1). Comparison of amino acid sequences between chicken and mammalian LILRB4–5 showed 17 to 62% and 19 to 29% similarity, respectively (Table 1). Moreover, phylogenetic analysis showed that the LILRB4–5 genes were closely associated with their corresponding genes from other species. Together with the high degree of sequence similarity, this indicates that the LILRB4R, -B5R, and LILRB4S, -B5S amino acids, which were isolated from the resistant and sensitive lines 6.3 and 7.2, respectively, are family genes and different in only functional and ITIM motif (Figure 1A). Thus, the LILRB4R, LILRB4S, LILRB5R, and LILRB5S genes are new LILRB4–5 variants in chicken.

## Structure and Potential Ligand Binding Properties of LILRB4-5 Proteins

The structure included a signal peptide, 2 Ig domains ($L^{23}$-$D^{116}$ and $Y^{119}$-$V^{212}/T^{213}$) with 2 N-glycosylation

**Table 1.** Similarities (upper) and identities (below) of chicken LILRB4 and LILRB5 genes in 2 genetically disparate chicken lines to those of other species.

| Species | Genes | Chicken B4R | Chicken B4S | Human B4 | Chimp B4 | Mouse B4 | Monkey B4 | Chicken B5R | Chicken B5S | Human B5 | Chimp B5 | Monkey B5 | Acc |
|---|---|---|---|---|---|---|---|---|---|---|---|---|---|
| Chicken | B4R | | 98.2 | 26.23 | 25.61 | 20.06 | 25.92 | 84.7 | 84.5 | 26.23 | 26.54 | 26.23 | Transcript ID |
| Chicken | B4S | 95.7 | | 25.92 | 25.3 | 19.13 | 25 | 84.1 | 83.9 | 25 | 25.3 | 25.92 | Transcript ID |
| Human | B4 | 49.6 | 49.5 | | 96.45 | 59.49 | 83.65 | 49.9 | 49.9 | 41.82 | 42.12 | 43 | NP_0,012,65356 |
| Chimpanzee | B4 | 57.1 | 57 | 90.57 | | 67.15 | 91.01 | 57.3 | 57.3 | 40.79 | 44.47 | 45.65 | NP_0,010,09045 |
| Mouse | B4 | 62.4 | 61.9 | 42.68 | 43.28 | | 43.58 | 62.2 | 62.3 | 36.71 | 38.5 | 39.1 | NP_03,8560 |
| Monkey | B4 | 57.1 | 56.7 | 81.97 | 81.72 | 67.59 | | 58.2 | 58.2 | 40.5 | 44.18 | 45.8 | NP_0,010,35766 |
| Chicken | B5R | 63 | 62 | 27.16 | 26.23 | 20.37 | 27.77 | | 99.4 | 28.08 | 27.77 | 27.77 | Transcript ID |
| Chicken | B5S | 63.9 | 63 | 27.46 | 26.54 | 20.67 | 28.08 | 97.8 | | 29.01 | 28.7 | 28.7 | Transcript ID |
| Human | B5 | 16.1 | 15.8 | 57.94 | 64.55 | 22.97 | 64.46 | 17.7 | 17.8 | | 93.93 | 81.88 | NP_0,012,91386 |
| Chimpanzee | B5 | 20.5 | 20.2 | 57.49 | 64.3 | 28.27 | 63.7 | 21.9 | 22.1 | 90.72 | | 86.89 | NP_0,010,09027 |
| Monkey | B5 | 21.9 | 21.9 | 57.27 | 64.55 | 29.6 | 65.22 | 23 | 23.1 | 84.38 | 85.48 | | XP_0,091,93549 |
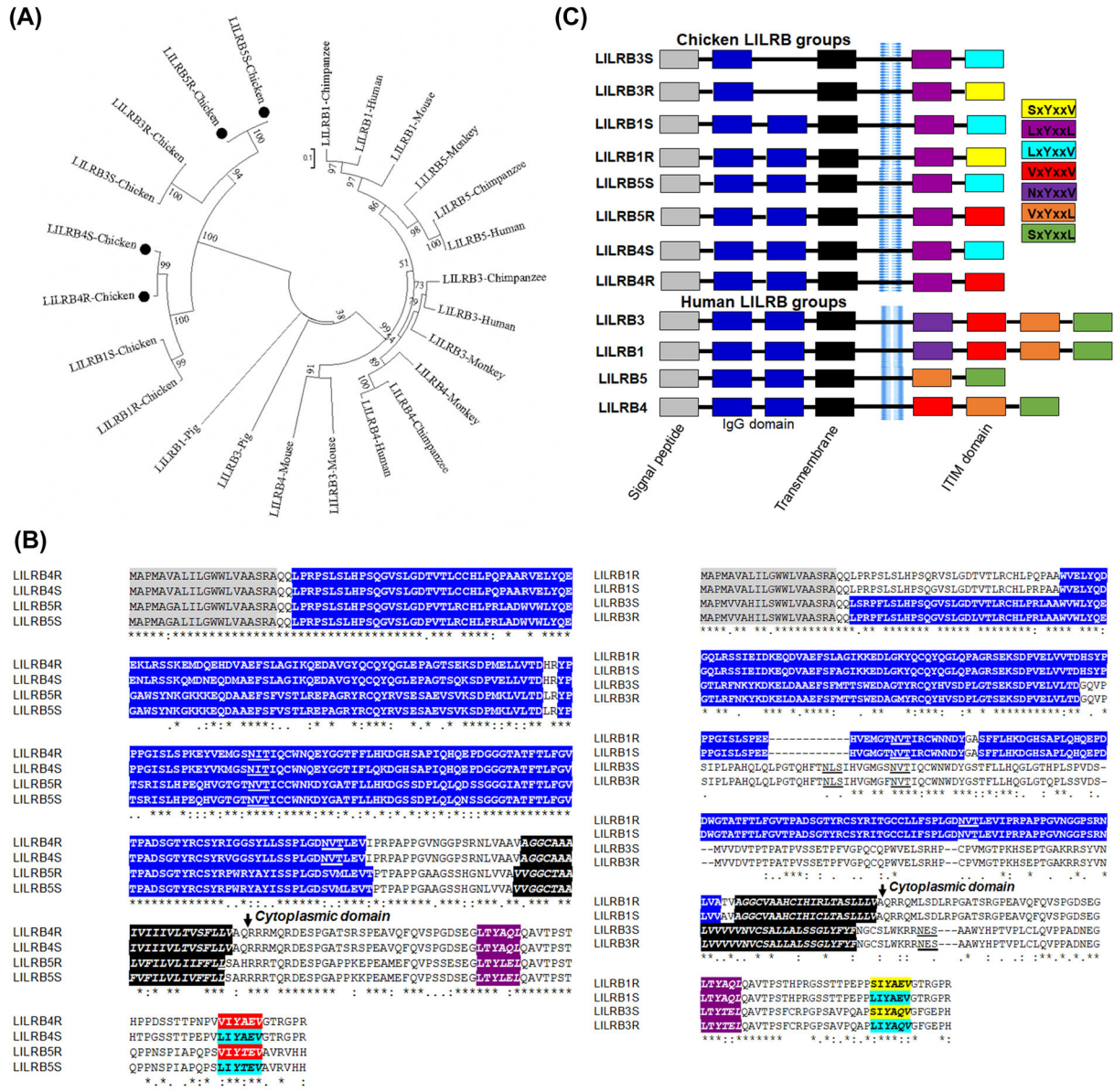
**Figure 1. Genetic analysis of LILRB4–5 genes identified from two genetically disparate chicken lines.** (**A**) Phylogenetic tree indicating the relationship between the chicken LILRB4–5 amino acid sequences and those from other vertebrates; (**B**) Multiple alignments of the predicted LILRB4–5 genes from the 2 chicken lines were performed using the ClustalX program. Amino acid sequence alignment of chicken LILRB4–5 genes together with human LILRB4–5 genes is shown. Signal peptide, an immunoglobulin domain, N-linked glycosylation sites, transmembrane and ITIM domain are indicated (**C**) Predicted structures of chicken LILRB4–5 genes compared with those of the known human LILRB4–5 genes.

($N^{137}$ and $N^{207}$) sites for LILRB4 and one N-glycosylation ($N^{137}$) site for LILRB5, transmembrane domain, and cytoplasmic domain with two ITIM motifs (Figure 1B). Based on the presence or absence of ITIM motifs, the signaling domains found in the chicken LILRB4–5 were conserved with those found in humans. The human LILRB4–5 contain 2–3 ITIMs with the VxYxxL and SxYxxL motifs being present on all of the receptors, whereas the chicken LILRB4–5 contain 2 ITIMs, with LxYxxL being present on every receptor (Figure 1C). Based on this, it is suggested that human LILRB4–5 may regulate or interact with more molecules than the chicken LILRB4–5.

Furthermore, the second ITIM motifs were different between the LILRB4–5 isolated from the 2 chicken lines; the motif VxYxxV was observed in the resistant line 6.3 (LILRB4R, LILRB5R), while the motif LxYxxV was present in the chicken susceptible line 7.2 (LILRB4S, LILRB5S) (Figure 1C). This suggests that the LILRB4–5 in both lines might show differences in their regulation of innate immunity. Further, similar to human ITIMs that also bind to the cytosolic tyrosine kinases SHP-1 and SHP-2 (Burshtyn et al., 1997), the ITIM motifs in the 2 chicken lines may be associated with tyrosine kinases and subsequent regulation of signaling pathway. Based on our observations, we

**Table 2.** Candidate binding ligands of LILRB4 and LILRB5 genes in 2 genetically disparate chicken lines that were predicted using the RaptorX web server.

| Name | Ligand | Binding residues | Domain | P-value | Binding with | References |
|---|---|---|---|---|---|---|
| LILRB4R | HOP | $R^{54}$ $E^{56}$ $Y^{58}$ $Q^{96}$ $L^{98}$ $T^{103}$ | 1 to 120 | 1.47E-07 | NI | |
| | NAG | $Q^{154}$ $D^{156}$ $S^{159}$ $R^{189}$ $L^{204}$ | 121 to 324 | 1.46E-06 | MHC class I, $\beta$2m | (Rudolph et al., 2001; Schiefner et al., 2009) |
| LILRB4S | IDO | $S^{37}$ $L^{38}$ $T^{115}$ $D^{116}$ $P^{203}$ $L^{204}$ | 1 to 218 | 3.31E-10 | MHC class I | (Rudolph et al., 2001) |
| LILRB5R | NAG | $L^{23}$ $P^{24}$ $R^{25}$ $S^{104}$ $V^{105}$ $K^{106}$ | 1 to 120 | 3.12E-07 | MHC class I, $\beta$2m | (Rudolph et al., 2001; Schiefner et al., 2009) |
| | GOL | $G^{148}$ $A^{149}$ $T^{150}$ $I^{172}$ $R^{193}$ $W^{195}$ | 121 to 324 | 1.54E-04 | MHC class I, $\beta$2m | (Hulsmeyer et al., 2004; Glithero et al., 2006) |
| LILRB5S | NAG | $L^{23}$ $P^{24}$ $R^{25}$ $S^{104}$ $V^{105}$ $K^{106}$ | 1 to 120 | 1.14E-07 | MHC class I, $\beta$2m | (Rudolph et al., 2001; Schiefner et al., 2009) |
| | SO4 | $T^{150}$ $L^{152}$ $R^{193}$ $W^{195}$ $A^{198}$ | 121 to 252 | 1.98E-04 | MHC class I, $\beta$2m | (Holmes et al., 2002; Uchtenhagen et al., 2013) |

suggest that the variants LILRB4–5 are largely similar in structure and function to those present in humans but may differ in their ligand-binding sites.

The ligands for LILRB4–5 can play a key role to clarify the function of LILRB4–5. In humans, LILRB4–5 have multiple ligands including MHC class I molecules (Jones et al., 2011; Zhang et al., 2015b). In this study, we used the RaptorX web server to screen candidate ligands of LILRB4R, -B4S, -B5R, and -B5S and to predict their function. The ligands of LILRB4–5 were mapped and searched using the RCSB protein data bank and in a public repository. The results showed that at least one of the candidate ligands for each of the LILRB4–5 genes was MHC-class I and $\beta$2m antigen (Table 2 and Figure S2). Comparison of the binding residues between the LILRB4–5 genes of the two chicken lines suggested that the degree of binding to MHC class I and $\beta$2m may differ between the 2 lines.

## MHC-class I and $\beta$2-microglobulin Heavy Chain Binds to LILRB4-5

Next, eGFP-linked with LILRB4R, -B4S, -B5R, or -B5S and mock control were transfected into HD11 cell line. Firstly, we determined the transfection efficiency by flow cytometry and fluorescent microscopy (Figure S2A) followed by fluorescence-activated cell sorting (**FACS**). The transfection efficiency was >85% for all as determined by FACS (Figure S2A). The LILRB4–5 protein expression was then determined by western blotting. As shown in Figure S2B, a single band was detected by anti-eGFP mAb in all of the transfected HD11 cell lines. Taken together, our data demonstrate that LILRB4–5 protein was expressed in HD11 cell line using our vector (Figure S2B). Moreover, the results of cytotoxicity analysis showed that the proliferation of HD11 cells was not significantly inhibited or enhanced after transfection with the pcDNA3-eGFP vector containing the CDS of LILRB4R, -B4S, -B5R, or -B5S (Figure S2B). The concentration of NO was significantly higher in LILRB4–5-eGFP-transfected than in the control group (Figure S2B), suggesting that constitutive expression of LILRB4–5 genes may induce intracellular production of reactive oxygen species in the form of NO.

In humans, LILRB4–5 was reported to bind to MHC class I and $\beta$2m (Jones et al., 2011; Zhang et al., 2015b). To clarify if this is also true for the newly identified LILRB4–5 variants, we generated transfected HD11 cells with eGFP-linked with LILRB4R, -B4S, -B5R, or -B5S or control and evaluated the binding of LILRB4–5 with MHC class I and $\beta$2m (Figure 2). As predicted, the gene expression pattern was dramatically different between cells transfected with GFP alone and GFP-linked with LILRB4–5. Firstly, immunoprecipitation analysis confirmed that LILRB4–5 binds to MHC class I and $\beta$2m (Figure 2). The LILRB4R, -B4S, -B5R, and -B5S immunoprecipitates contained approximately 42- and 14-kDa proteins as shown in the anti-MHC class I and $\beta$2m blot, respectively (Figure 2). The expression of LILRB4R, -B4S, -B5R, and -B5S immunoprecipitated with MHC class I was higher than that with $\beta$2m. Furthermore, MHC-1 and $\beta$2m could precipitate higher amounts of LILRB4R, -B5R than did LILRB4S, -B5S, suggesting that the MHC class I and $\beta$2m association with LILRB4R, -B4S, -B5R, and -B5S was receptor-dependent (Figure 2).

Secondly, the genes mostly upregulated by the active forms of LILRB4–5 genes were the various members of the MHC class I (*HLA-A, BF-I,* and *BF-IV*) family as well as other genes involved in class I antigen presentation and processing, such as *$\beta$2m, TAP1,* and *TAP2* (Figure 2), as confirmed by quantitative real-time PCR using cells transfected with GFP-linked LILRB4–5 genes or GFP alone (Figure 2). Further, the upregulation of the MHC class I family genes and related genes was higher by LILRB4R, -B5R than by LILRB4S and -B5S. Specifically, the expression of $\beta$2m mRNA was markedly increased by 19.6-, 16.3-, 32.1, and 12.1-fold in HD11 cell line transfected with LILRB4R, -B4S, -B5R, and -B5S, respectively. The expression of *BF-I, BF-IV,* and *HLA-A* was highly upregulated due to LILRB4R by 42.7-, 174.8-, and 78.0-fold, respectively. The expression of MHC class I related genes such as *TAP-1* and *TAP-2* was significantly upregulated by 86.9- and 72.6-fold by LILRB4R and LILRB5R, respectively (Figure 2).

Finally, flow cytometry analysis using MHC class I and $\beta$2m antibodies confirmed an increase in the surface expression of MHC class I in cells transfected with LILRB4–5. Particularly, constitutive expression of LILRB4R, -B4S, -B5R and -B5S resulted in increased
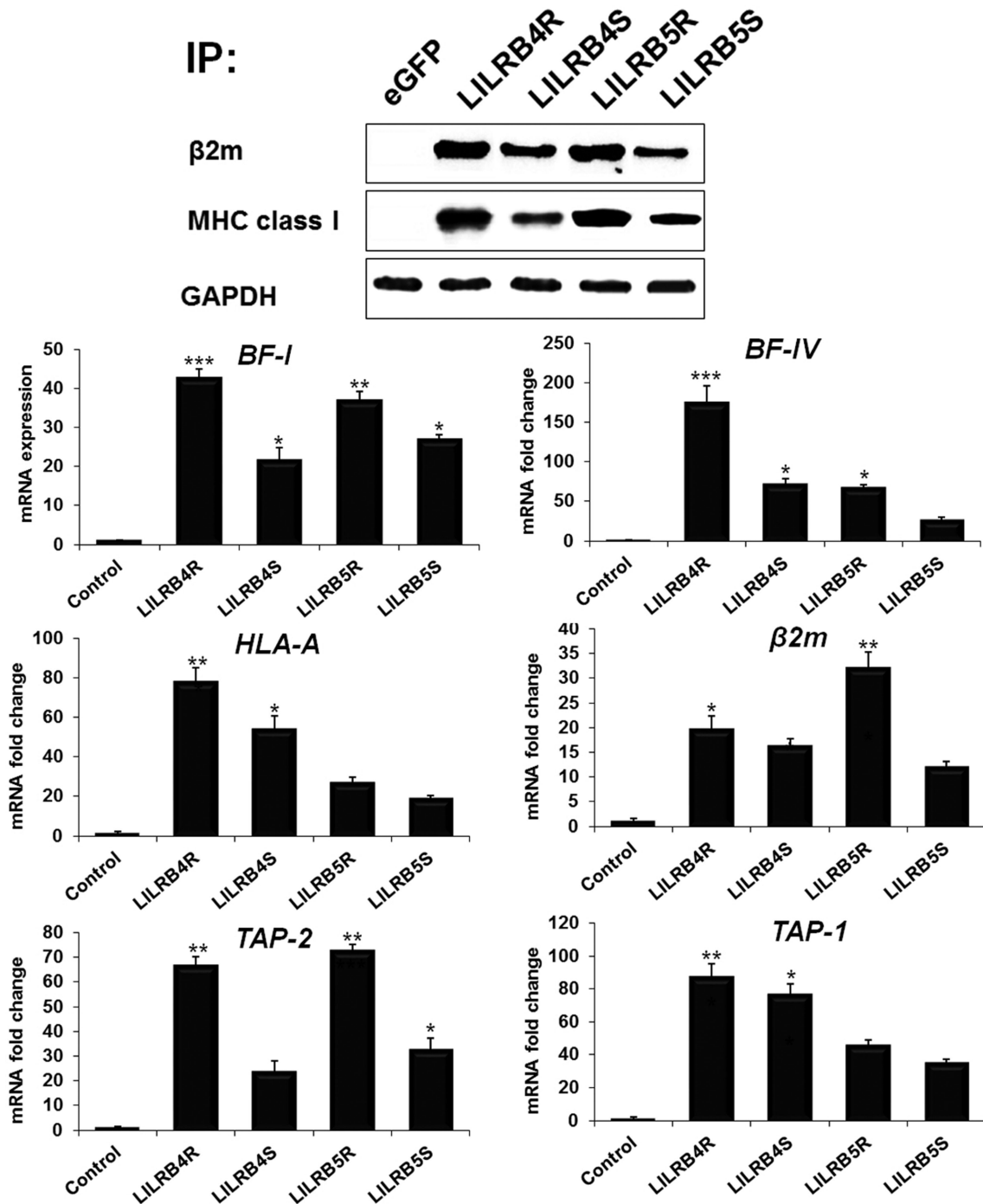
**Figure 2. LILRB4–5 glycoprotein associated with MHC class I and β2m.** *Top panel*, HD11 cells transfected with LILRB4–5 genes from the two chicken were lysed and then immunoprecipitated with the MHC class I and β2m mAb, separated by SDS-PAGE, and immunoblotted with secondary antibody. *Bottom panel*, changes in mRNA levels of MHC class I family and related genes upon transfection with LILRB4–5 genes were detected by qRT-PCR. Data are presented as the mean ± SEM ($n = 3$) of 3 independent experiments: $*P < 0.05$, $**P < 0.01$, and $***P < 0.001$.

percentages of cells showing MHC class I by 51.8, 41.2, 31.2, 19.9%, respectively, and those expressing β2m by 29.5, 24.2, 33.1, and 28.4%, respectively (Figure 3). Together, these data indicate that LILRB4–5 genes induce the expression of MHC class I and related genes involved in MHC class I antigen presentation, although the level of binding between LILRB4–5 and MHC class I and related genes seemed to be higher with the proteins from line 6.3 than with those from line 7.2.

## Association of SHP-2 with Phosphorylated LILRB4-5 Molecules

The tyrosine phosphatase SHP-2 associates with phosphorylated LILRB group in T cells, B cells, macrophage cells, and natural killer cells (Kang et al., 2015). To determine whether the newly identified LILRB4–5 variants associated with SHP-2, we examined their tyrosine phosphorylation profile in
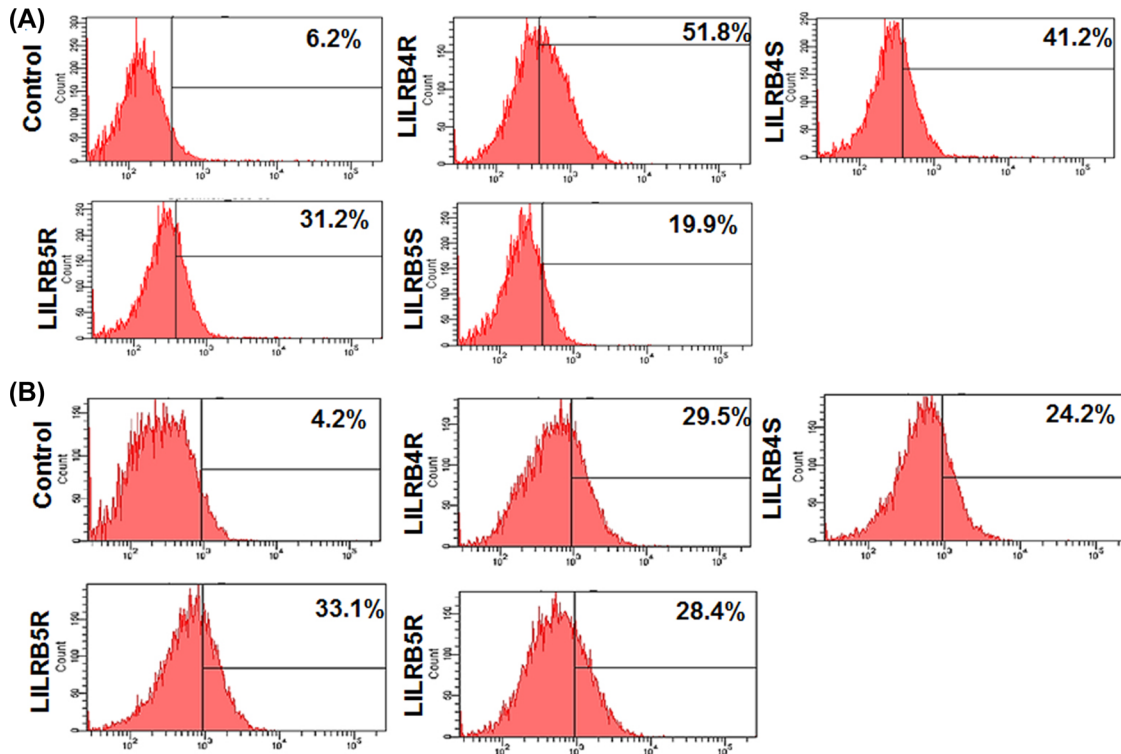
**Figure 3. MHC class I and $\beta$2m mAb bind to LILRB4–5 genes from two genetically distinct chicken lines.** HD11 cells transfected with eGFP and eGFP-tagged constructs of LILRB4R, -B4S, -B5R, and -B5S stained with (**A**) MHC class I or (**B**) or $\beta$2m labeled with PE. Binding was assessed by FACS analysis.

LILRB4–5-eGFP-transfected HD11 cell line (Figure 4). Flow cytometry analysis using an SHP-2 (phosphor-Tyr$^{542}$) antibody confirmed an increase in SHP-2 protein expression in cells transfected with LILRB4–5 genes; the expression levels of SHP-2 associated with LILRB4R, -B4S, -B5R, and -B5S were comparable, with 19.8, 15.9, 21.4, and 20.9% percentage of cells showing increased SHP-2 expression, respectively (Figure 4A). It is interesting that the levels of SHP-2 associated with the LILRB4–5 identified in line 6.3 were higher than those in line 7.2 (Figure 4A). A protein of approximately 66 kDa (Figure 4B), corresponding to LILRB4R, -B4S, -B5R, and -B5S, could be detected in anti-SHP-2 immunoprecipitates, but not in immunoprecipitates generated with mock control. These results suggest that tyrosine phosphorylation is essential for SHP-2 binding to LILRB4R, -B4S, -B5R, and -B5S. Finally, quantitative real-time PCR analysis showed elevated levels of SHP-2 expression in cells transfected with the GFP-linked LILRB4–5 genes (Figure 4B), with the expression of *SHP-2* mRNA being the highest in LILRB5R-transfected cells compared with that in mock control. Furthermore, in comparison to genes from line 7.2, the transfected genes from line 6.3 resulted in higher expression of *SHP-2* mRNA by 34.4-, 24.4-, 76.9-, and 44.9-fold for LILRB4R, -B4S, -B5R, and -B5S, respectively (Figure 4B). Thus, we concluded that LILRB4R, -B4S, -B5R, and -B5S in macrophages were constitutively tyrosine-phosphorylated and associated with SHP-2.

## LILRB4-5 Significantly Promoted the Phosphorylation of Signaling Transduction Molecules STAT and JAK

Next, we examined whether the LILRB4–5 genes affected the JAK/STAT signaling pathway, which plays an important role in immune responses. Here, we observed that STAT1 (p-Ser$^{727}$), STAT3 (p-Ser$^{727}$), and JAK2 (p-Tyr$^{1007}$/Tyr$^{1008}$) were phosphorylated in response to constitutive expression of LILRB4–5 genes in HD11 cell lines. In addition, the un-phosphorylated (*STAT1/3, JAK2*, and *TYK2*) protein levels, as detected by western blotting, were higher for LILRB4R and -B5R-transfected cells than for -B4S and -B4S-transfected cells (Figure 5A). Together, our observations indicate that LILRB4–5 genes can activate the JAK/STAT signaling pathway in the two genetically disparate chicken lines.

The mRNA expression of the JAK/STAT signaling pathway genes was evaluated by qRT-PCR and the results are shown in Figure 5B. *STAT1* and *STAT3* mRNA relative expression was increased in LILRB4R transfected cells by 150.5- and 31.0-fold, and in LILRB5R-transfected cells by 94.9 to 38.0-fold, while cells transfected with LILRB4S and LILRB5S showed 63.2- and 28.0-fold, and 24.9 and 17.3-fold increases, respectively (Figure 5B). Similarly, *JAK2* and *TYK2* mRNA was more highly expressed in cells transfected with LILRB5R (32-, 142.4-fold) and LILRB4R (19.6-, 103.9-fold) than in cells transfected with
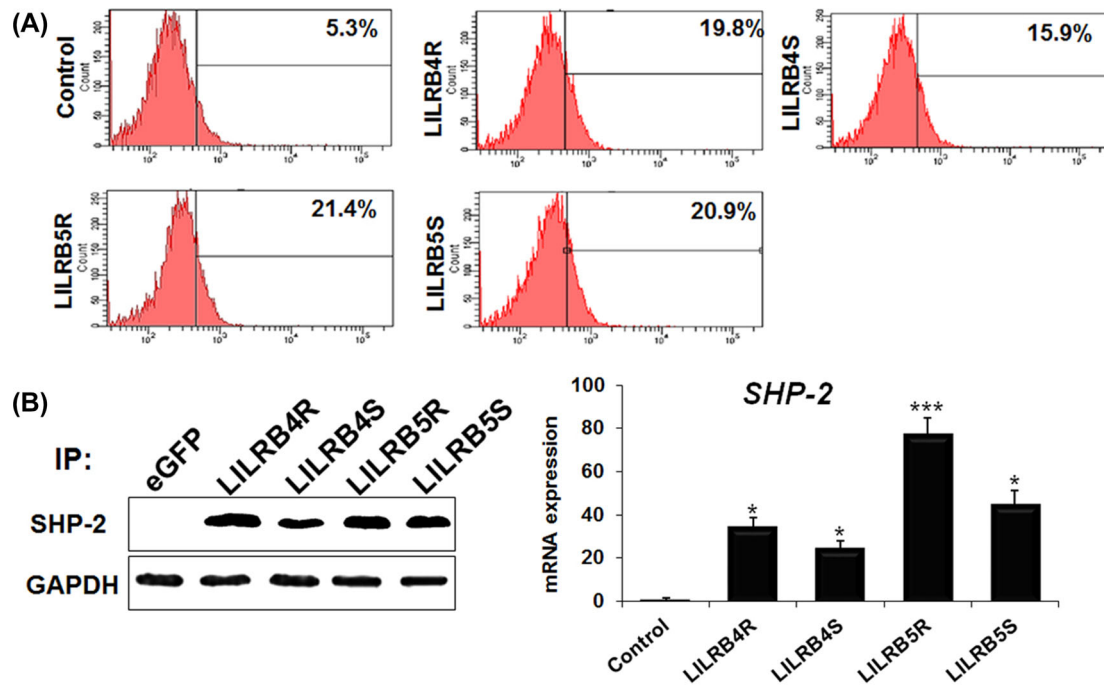
**Figure 4. LILRB4R, -B4S, -B5R, and -B5S glycoprotein associated with SHP-2.** (**A**) HD11 cells transfected with eGFP and eGFP-tagged constructs of LILRB4R, -B4S, -B5R, and -B5S stained with SHP-2 mAb and then by Alexa Fluor® 488 labeled anti-rabbit secondary antibody. Binding was assessed by FACS analysis. (**B**) Immunoprecipitation analysis of LILRB4–5 association with SHP-2 (**Left**) and changes in SHP-2 mRNA levels in transfection by LILRB4–5 were detected by qRT-PCR. Data are presented as the mean ± SEM ($n = 3$) of 3 independent experiments: *$P < 0.05$, **$P < 0.01$, and ***$P < 0.001$.

LILRB4S (16.3-, 70.4-fold) and -B5S (12-, 92.4-fold), respectively (Figure 5B). We also evaluated suppressor of cytokine signaling 1 (**SOCS1**) expression by western blot and qRT-PCR analysis (Figure 5B). SOCS1 protein was strongly detected in LILRB5R-transfected cells, and qRT-PCR analysis showed strong upregulation of *SOCS1* mRNA genes in cells transfected with LILRB4–5 genes from line 6.3 (LILRB5R showed a 31.8- fold increase) compared with those in line 7.2 (LILRB4S showed a 16.4-fold increase) (Figure 5B).

## LILRB4-5 Significantly Upregulated Cytokine mRNA Levels

Next, we determined the levels of cytokine gene expression in transfected HD11 cell lines using qRT-PCR (Figure 6). The mRNA levels of chemokines *CCL-4, CXCL-13*, and *CXCL-14* were significantly increased upon constitutive expression of LILRB4–5 genes from both chicken lines. Particularly, LILRB5R-transfection showed the highest upregulation, and the increase in chemokine expression was higher in cells transfected with LILRB4R and -B5R than in those transfected with -B4S and -B5S (Figure 6). Similarly, the levels of Th1-type cytokines, *IFN-α, IFN-β, IL-1β*, and *IL-6* mRNA, were also dramatically upregulated by LILRB4–5 genes. *IFN-β* and *IL-1β* mRNA was highly expressed with a 116.0- and 145.0-fold increase, respectively, in LILRB4R-transfected cells. The expression of *IFN-α* and *IL-6* mRNA showed a 103.4- and 149.4-fold increase in LILRB5R-transfected cells (Figure 6). The effects of constitutive expression of LILRB4R, -B4S, -B5R, and -B5S on the Th-2 type cytokines (*IL-4, IL-10*), Treg cytokine (*TGF-β4*), and proinflammatory mediator (*LITAF*) were also examined, in which *TGF-β4, IL-4*, and *IL-10* mRNA was strongly upregulated by 146.5-, 108.0-, and 216.3-fold in LILRB4R-transfected cells, respectively, while *LITAF* mRNA was increased by 77.5-fold after transfection with LILRB5R (Figure 6). Moreover, the Th17 cytokine (*IL-17F*) was also upregulated by 102.7-fold after transfection with LILRB5R (Figure 6). Thus, the chemokines were more highly upregulated by the genes from line 6.3 compared with those from line 7.2 (Figure 6). Together, these results suggest that LILRB4–5 genes may promote the induction of Th1/2/17 cytokine production *in vitro* on activated macrophage cell lines and that the variants from the resistant chicken cell line 6.3 have a stronger effect than those from the susceptible line 7.2.

## LILRB4-5 Induced Cytokine Protein Production

The expression of *IFN-γ* mRNA was significantly increased in LILRB4R, -B4S, -B5R, and -B5S transfected cells compared with that in mock control by 44.5-, 15.3-, 42.4-, and 27.9-fold, respectively (Figure 7). To determine if this increase corresponded with increased IFN-γ
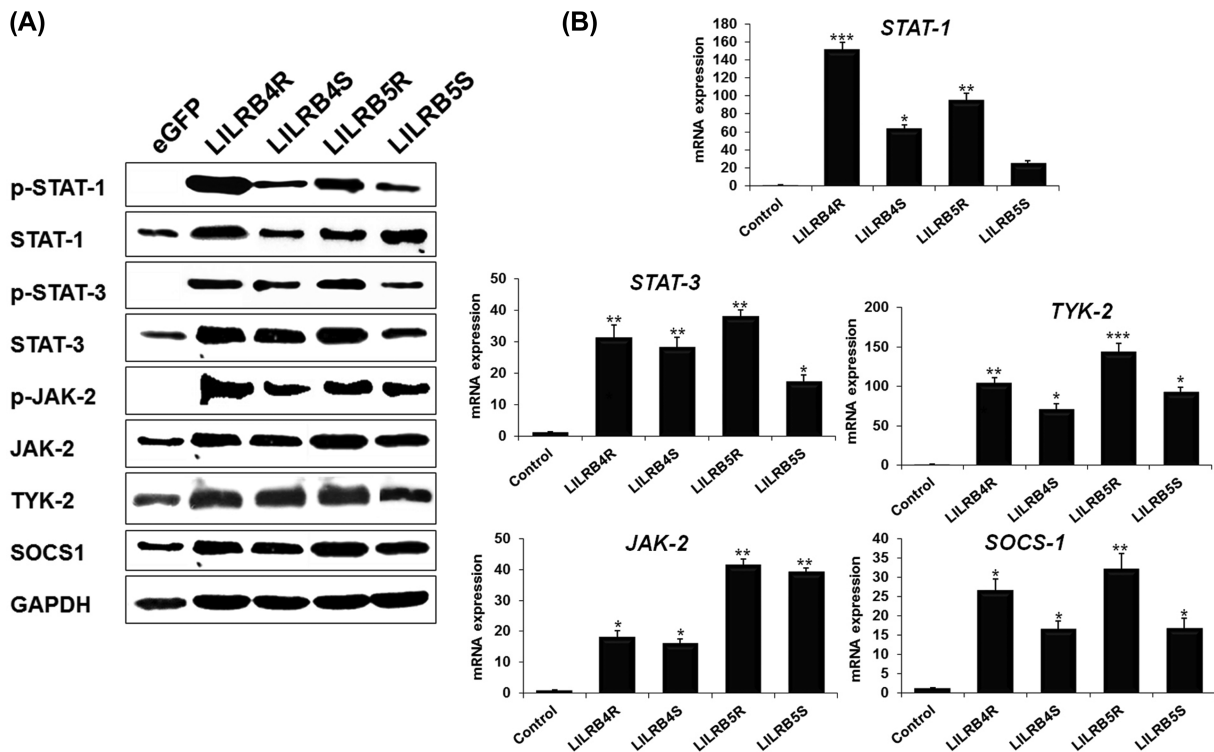
**(A)**



**(B)**



**Figure 5. LILRB4R, -B4S, -B5R, and -B5S glycoprotein regulated the JAK-STAT signaling pathway.** (**A**) Western blotting results of JAK2/TYK2, STAT1/3, and SOCS1 after LILRB4–5 transfection of HD11 cell line. (**B**) Changes in mRNA levels of JAK2/TYK2, STAT1/3 and SOCS1 genes after LILRB4–5 transfection in HD11 cell line were detected by qRT-PCR. Data are presented as the mean $\pm$ SEM ($n = 3$) of 3 independent experiments: *$P < 0.05$, **$P < 0.01$, and ***$P < 0.001$.

protein expression, we measured IFN-$\gamma$ protein levels in the supernatant of LILRB4-5-transfected cells by enzyme-linked immunosorbent assay (**ELISA**). Analysis revealed significantly higher IFN-$\gamma$ protein levels of 1312, 537, 1461, and 812 ng/mL, in LILRB4R, -B4S, -B5R, and -B5S transfected cells, respectively, than in the mock control, which showed 55 ng/mL IFN-$\gamma$ level (Figure 7). Similarly, the mRNA as well as protein expression levels of the Th17 cytokine (IL-17A and IL-12p40) were also upregulated by the LILRB4–5 genes (Figure 7). Moreover, constitutive expression of LILRB4R and LILRB5R resulted in a higher production of IFN-$\gamma$, IL-17A, and IL-12p40 than that of LILRB4S and LILRB5S. The association between LILRB4–5 and IFN-$\gamma$/Th17 cytokines may represent a promising new therapeutic target.

## DISCUSSION

In this study, we used a bioinformatics approach along with in vitro assays to identify and characterize novel LILRB4–5 gene variants isolated from 2 genetically disparate chicken lines. Our initial search yielded 4 transcripts as potential LILRB4–5 genes in chicken line 6.3 and line 7.2, which were then analyzed using phylogeny alongside other structurally similar receptor families belonging to the Ig-superfamily. Comparison of amino acid identities and similarities between LILRB4 and LILRB5 in line 6.3 to those in line 7.2 and also to

mammalian proteins showed a 95 to 97%, 98 to 99%, 17 to 62%, and 19 to 9% similarity, respectively. Moreover, phylogenetic analysis based on amino acid similarity placed the LILRB4R, -B4S, -B5R, and -B5S together with members of the mammalian LILRB4–5 genes, indicating that these chicken variants were closely associated with similar genes from other species and represent novel homologs in chicken LILRB family. The human LILRB4–5 receptors contain between 2 and 3 canonical and permissive ITIMs, in which the VxYxxL and SxYxxL motifs are present on every receptor (Vivier and Daeron, 1997), whereas the LILRB4R, -B4S and -B5R, -B5S receptors in our study were found to contain only one canonical ITIM motif (LxYxxL) on each receptor. This indicates that the human LILRB4–5 possibly show a greater diversity of signaling abilities than the chicken LILRB4–5 genes. Our observations further suggested that the LILRB4–5 genes could be subdivided into two groups: transmembrane molecules with 2 ITIM motifs (LxYxxL and VxYxxV) in resistant line 6.3 and those with 2 ITIM motifs (LxYxxL and LxYxxV) in susceptible line 7.2, suggesting that the genes from the 2 chicken lines may possess different signaling abilities. Interestingly, at least one of the motifs in both groups contained the sequence V/YxxL/V, which has been shown to be the consensus sequence for binding the SH2 domains of the SHP-1 or SHP-2 phosphatase. A previous report showed that tyrosine-phosphorylated LILRB4–5 associates and coimmunoprecipitates with
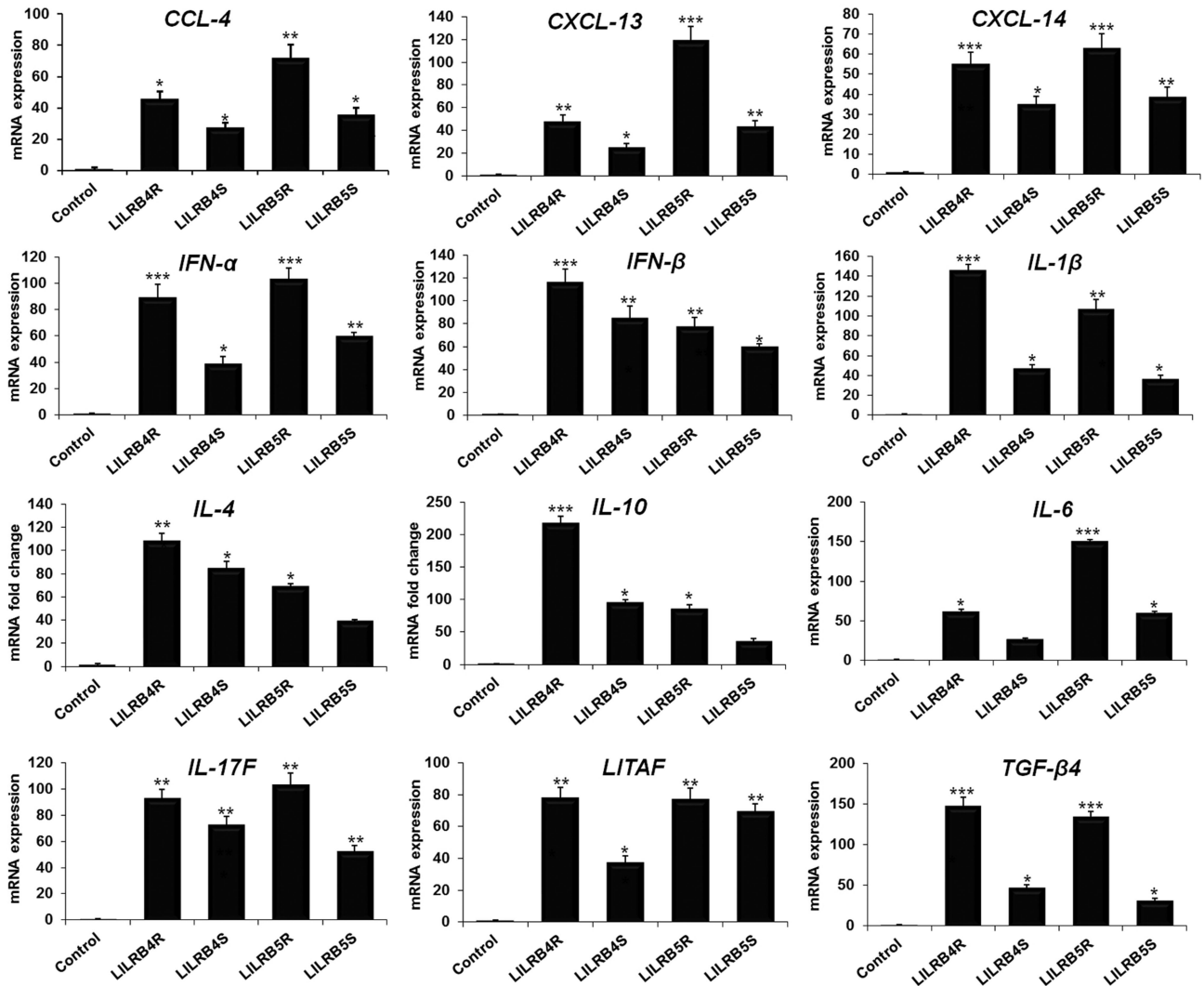
**Figure 6.** Cytokine expression induced by LILRB4R, -B4S, -B5R, and -B5S in HD11 cell lines after transfection. Data are presented as the mean ± SEM ($n = 3$) of 3 independent experiments: *$P < 0.05$, **$P < 0.01$, and ***$P < 0.001$.

SHP-1 and SHP-2 (Colonna et al., 1998). Evidence from other immunoreceptors suggests that the phosphorylation of such motifs generates binding sites for other signaling molecules, including SHIP, SHP-1, and SHP-2 (Colonna et al., 1998). To demonstrate this point, we analyzed the level of association of LILRB4–5 with SHP-2 by immunoprecipitation, FACS analysis, and qRT-PCR, in the 2 chicken lines. Our results indicated that the association of LILRB4–5 from the resistant line 6.3 with SHP-2 was significantly higher than that with proteins from line 7.2. Recently, it was suggested that SHP-2, a cytoplasmic SH2 domain-containing protein tyrosine phosphatase, is involved in the signaling pathways of a variety of growth factors and cytokines such as JAK-STAT and MAPK signaling pathways, and plays an important role in transducing signal relay from the cell surface to the nucleus, and in intracellular regulation of cell proliferation and differentiation (Burshtyn et al., 1997). Thus, LILRB4–5 genes from the 2 chicken lines may differentially regulate signaling pathways and cytokine production.

In humans, the binding of LILRB4–5 to HLA-A, -B, and -C, and other non-classical class I molecules, such as HLA-E, HLA-G, and HLA-F, is currently being evaluated in several cell types (Jones et al., 2011; Zhang et al., 2015b). Our predictive analysis indicated that each of the LILRB4–5 genes included the candidate ligands MHC class I and $\beta$2m antigen. *In vivo* analysis by immunoprecipitation, FACS, and qRT-PCR indicated that LILRB4–5 from the 2 chicken lines strongly bind to MHC class I and $\beta$2m, with binding to MHC class I being significantly higher than to $\beta$2m. Additionally, binding of the proteins from line 6.3 was dramatically higher than that of proteins from line 7.2. Moreover, LILRB4–5 genes from both chicken lines significantly upregulated (more than 50-fold) the MHC class I-related genes such as *TAP-1* and *TAP-2*, which are essential for antigen presentation by the MHC class I pathway. This finding that MHC class I is recognized by the inhibitory receptors LILRB4–5 expressed on macrophage cells represents an expansion of the concept of self-recognition. Taken together, our findings show that LILRB4–5
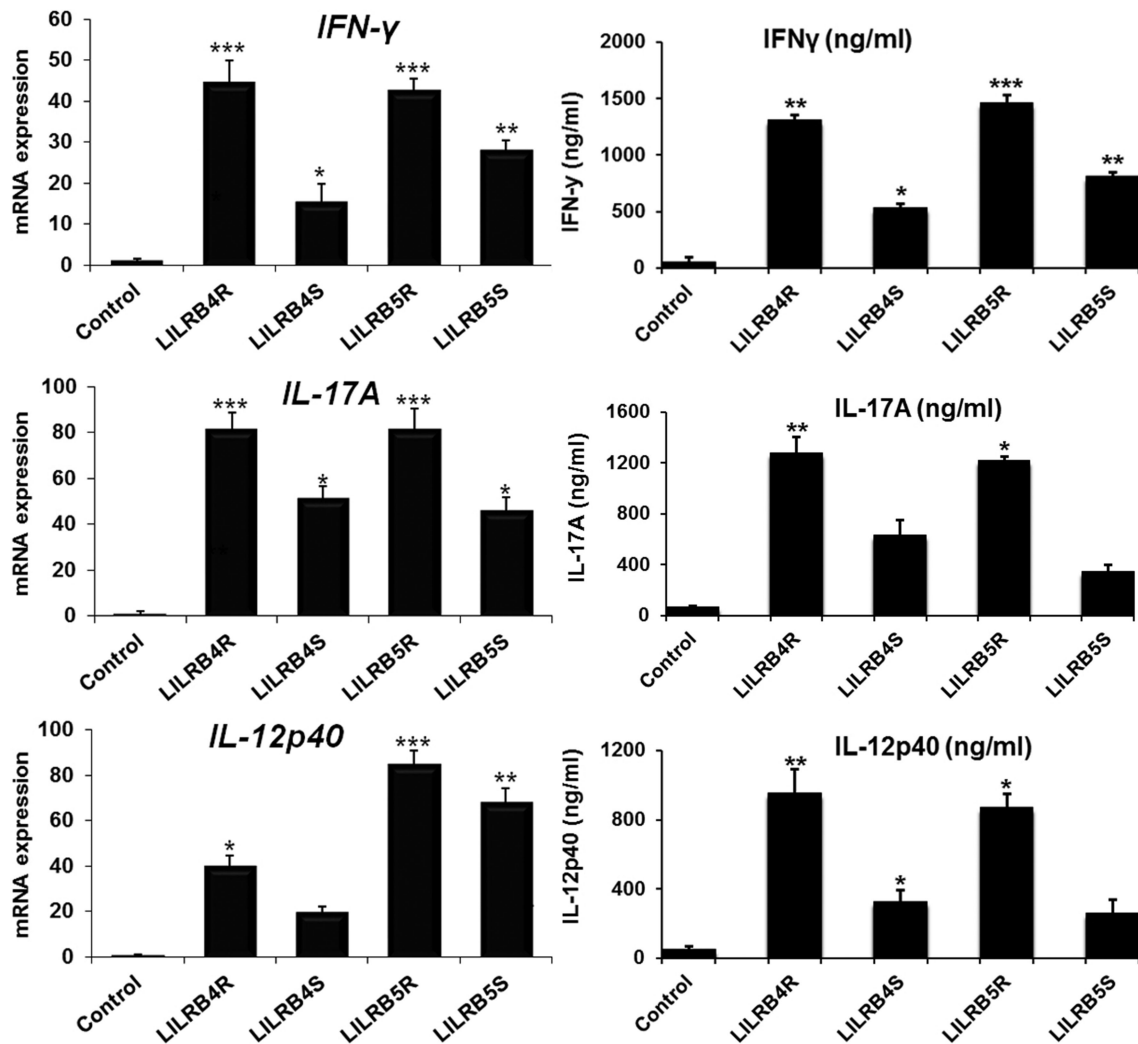
**Figure 7.** Level of cytokine protein expression induced by LILRB4R, -B4S, -B5R, and -B5S in HD11 cell lines after transfection. Data are presented as the mean $\pm$ SEM ($n = 3$) of 3 independent experiments: $*P < 0.05$, $**P < 0.01$, and $***P < 0.001$.

genes are necessary and sufficient for the induction of MHC class I expression. Future analyses of the *in vivo* function of LILRB4–5 genes are required to reveal whether these two molecules play redundant or more exclusive roles in MHC class I-dependent immune responses.

A deeper understanding of the intracellular signal transduction pathways initiated by LILRB4–5 genes is necessary to know how the LILRB4–5 genes can activate immune-related gene expression. Here, we demonstrated that LILRB4–5 genes could induce the JAK/STAT signaling pathway, which plays a key role in multiple cytokine-induced responses (Finbloom and Larner, 1995). Moreover, LILRB4–5 proteins have been shown to regulate TLR activity (Brown et al., 2009), antigen-presenting phenotype, and cytokine production (Brown et al., 2009), thus demonstrating that LILRB4–5 proteins play an important role in the regulation of innate immune responses. In the current study, the increased level of STAT1 (p-Ser$^{727}$), STAT3 (p-Ser$^{727}$), and JAK2 (p-Tyr$^{1007}$/Tyr$^{1008}$) phosphorylated molecules, upregulation of un-phosphorylated

(STAT1/3, JAK2, TYK2, and SOCS1) molecules, and increased mRNA levels of STAT1/3, JAK2, TYK2, and SOCS1 in response to constitutive LILRB4–5 expression indicate that LILRB4–5 activate the JAK/STAT signaling pathway. Thus, our study provides the first evidence indicating the possible role of the JAK/STAT pathway in the signaling mechanism of chicken LILRB4–5 genes.

Our qRT-PCR analysis carried out for 3 chemokines (CCL-4, CXCL-13, and CXCL-14) and 12 cytokines (IL-1$\beta$, IL-4, IL-6, IL-10, IL-12p40, IL-17A, IL-17F, IFN-$\alpha$, IFN-$\beta$, IFN-$\gamma$, LITAF, and TGF$\beta$4), along with ELISA results for protein expression of Th1 (IFN-$\gamma$) and Th2 (IL-17A, IL-12, p40) indicated that these cytokines were more highly increased in cells transfected with LILRB4–5 genes from line 6.3 than in those from line 7.2. As previously reported, chemokines promote host resistance by mobilizing leukocytes and activating immune functions that kill, expel, or sequester pathogens (Chensue, 2001). IFN-$\alpha$, IFN-$\beta$, IFN-$\gamma$, and IL-17, highly produced from Th1 and Th17 cells, play important roles in resistance against

resistant pathogens and also increase expression of class I MHC molecules on cells, making them more resistant to pathogens (Vilcek and Feldmann, 2004). IFN and IL-17 also induce IL-1$\beta$, IL-6, LITAF, and TGF$\beta$4 mRNA production (Vilcek and Feldmann, 2004). Moreover, Th2 cytokine (IL-10) and Treg cytokine (TGF$\beta$4) mRNA has been reported to upregulate the cell surface expression of the inhibitory receptors on monocytes and dendritic cells and also the expression of IL-10 and TGF$\beta$4 to respond to pathogens such as HIV (Bashirova et al., 2014). Thus, the LILRB4–5 genes induce a distinct macrophage cell activation state characterized by the production of several chemokines and Th1, Th2, and Th17 cytokines, including CCL-4, CXCL-13, CXCL-14, IL-1$\beta$, IL-4, IL-6, IL-10, IL-12p40, IL-17A, IL-17F, IFN-$\alpha$, IFN-$\beta$, IFN-$\gamma$, LITAF, and TGF$\beta$4, which may be essential in the pathogenesis of diseases, highlighting the importance of this novel pathway in chicken disease.

In summary, this is the first report on the cloning, structural analysis, and function of the novel chicken LILRB4–5 genes, which were identified from two genetically distinct chicken lines. LILRB4–5 genes possess ITIM motifs in the cytoplasmic domain, which binds to the cytosolic tyrosine kinase SHP-2. Further, the LILRB4–5 genes bind to MHC class I and $\beta$2m as well as other genes involved in class I antigen presentation and processing and regulate immune responses. Importantly, LILRB4–5 genes induce the JAK/STAT signaling pathway and expression of chemokines and Th1, Th2, and Th17 cytokine genes.

## SUPPLEMENTARY DATA

Supplementary data are available at *Poultry Science* online.

**Table S1**. Gene ID, transcript ID, sequence length, location, and expression of chicken LILRB4–5 revealed by RNA-Seq.
**Table S2**. Primer sequences for cloning and real-time PCR analyses of cytokine expression levels.
**Figure S1.** Prediction of candidate ligand of LILRB4–5 genes in the 2 chicken lines. The structure and ligand-binding sites of the proteins were determined by molecular replacement using the program RaptorX web server.
**Figure S2.** Subcellular distribution of chicken LILRB4–5 genes in the 2 chicken lines. (**A**) HD11 cell lines were transiently transfected with an expression plasmid-encoding chicken LILRB4–5 fused to GFP, and after 48 h, FACS analysis was performed on GFP-positive cells (**bottom**). (**B**) Schematic representation of the LILRB4–5 gene expression constructs (**left**); CMV = human cytomegalovirus immediate early promoter; ORF = open reading frame; PolyA = bovine growth hormone polyadenylation site. Western blot analysis was performed with antibodies against GFP (**middle**) and the cytotoxicity of LILRB4R, -B4S, -B5R, and

-B5S linked eGFP vector transfected into HD11 cell line was determined by cell proliferation and NO production assays.

## REFERENCES

Bashirova, A. A., E. Martin-Gayo, D. C. Jones, Y. Qi, R. Apps, X. Gao, P. S. Burke, C. J. Taylor, J. Rogich, S. Wolinsky, J. H. Bream, P. Duggal, S. Hussain, J. Martinson, A. Weintrob, G. D. Kirk, J. Fellay, S. P. Buchbinder, J. J. Goedert, S. G. Deeks, F. Pereyra, J. Trowsdale, M. Lichterfeld, A. Telenti, B. D. Walker, R. L. Allen, M. Carrington, and X. G. Yu. 2014. LILRB2 interaction with HLA class I correlates with control of HIV-1 infection. PLos Genet. 10:e1004196. doi 10.1371/journal.pgen.1004196.

Bergamini, A., M. S. Chimenti, E. Baffari, M. D. Guarino, G. Gigliucci, C. Perricone, and R. Perricone. 2014. Downregulation of immunoglobulin-like transcript-4 (ILT4) in patients with psoriatic arthritis. PLoS One 9:e92018. doi 10.1371/journal.pone.0092018.

Brown, D. P., D. C. Jones, K. J. Anderson, N. Lapaque, R. A. Buerki, J. Trowsdale, and R. L. Allen. 2009. The inhibitory receptor LILRB4 (ILT3) modulates antigen presenting cell phenotype and, along with LILRB2 (ILT4), is upregulated in response to Salmonella infection. BMC Immunol. 10:56. doi 10.1186/1471-2172-10-56.

Burshtyn, D. N., W. Yang, T. Yi, and E. O. Long. 1997. A novel phosphotyrosine motif with a critical amino acid at position -2 for the SH2 domain-mediated activation of the tyrosine phosphatase SHP-1. J. Biol. Chem. 272:13066–13072.

Chensue, S. W. 2001. Molecular machinations: chemokine signals in host-pathogen interactions. Clin. Microbiol. Rev. 14:821–835, table of contents.

Colonna, M., J. Samaridis, M. Cella, L. Angman, R. L. Allen, C. A. O'Callaghan, R. Dunbar, G. S. Ogg, V. Cerundolo, and A. Rolink. 1998. Human myelomonocytic cells express an inhibitory receptor for classical and nonclassical MHC class I molecules. J. Immunol. 160:3096–3100.

Finbloom, D. S., and A. C. Larner. 1995. Regulation of the Jak/STAT signalling pathway. Cell. Signal. 7:739–745.

Glithero, A., J. Tormo, K. Doering, M. Kojima, E. Y. Jones, and T. Elliott. 2006. The crystal structure of H-2D(b) complexed with a partial peptide epitope suggests a major histocompatibility complex class I assembly intermediate. J. Biol. Chem. 281:12699–12704.

Hogan, L. E., D. C. Jones, and R. L. Allen. 2016. Expression of the innate immune receptor LILRB5 on monocytes is associated with mycobacteria exposure. Sci. Rep. 6, 21780; doi: 10.1038/srep21780.

Holmes, M. A., P. Li, E. W. Petersdorf, and R. K. Strong. 2002. Structural studies of allelic diversity of the MHC class I homolog MIC-B, a stress-inducible ligand for the activating immunoreceptor NKG2D. J. Immunol. 169:1395–1400.

Hulsmeyer, M., M. T. Fiorillo, F. Bettosini, R. Sorrentino, W. Saenger, A. Ziegler, and B. Uchanska-Ziegler. 2004. Dual, HLA-B27 subtype-dependent conformation of a self-peptide. J. Exp. Med. 199:271–281.

Jansen, C. A., D. A. van Haarlem, B. Sperling, P. J. van Kooten, E. de Vries, B. C. Viertlboeck, L. Vervelde, and T. W. Gobel. 2016. Identification of an activating chicken Ig-like receptor recognizing Avian influenza viruses. J. I. 197:4696–4703.

Jones, D. C., V. Kosmoliaptsis, R. Apps, N. Lapaque, I. Smith, A. Kono, C. Chang, L. H. Boyle, C. J. Taylor, J. Trowsdale, and

R. L. Allen. 2011. HLA class I allelic sequence and conformation regulate leukocyte Ig-like receptor binding. J. Immunol. 186:2990–2997.

Kang, X., J. Kim, M. Deng, S. John, H. Chen, G. Wu, H. Phan, and C. C. Zhang. 2016. Inhibitory leukocyte immunoglobulin-like receptors: immune checkpoint proteins and tumor sustaining factors. Cell Cycle 15: 25–40.

Kim, T., G. S. Vidal, M. Djurisic, C. M. William, M. E. Birnbaum, K. C. Garcia, B. T. Hyman, and C. J. Shatz. 2013. Human LilrB2 is a beta-amyloid receptor and its murine homolog PirB regulates synaptic plasticity in an Alzheimer's model. Science 341:1399–1404.

Klasing, K. C., and R. K. Peng. 1987. Influence of cell sources, stimulating agents, and incubation conditions on release of interleukin-1 from chicken macrophages. Dev. Comp. Immunol. 11:385–394.

Livak, K. J., and T. D. Schmittgen. 2001. Analysis of relative gene expression data using real-time quantitative PCR and the 2(-Delta Delta C(T)) Method. Methods 25:402–408.

Rothe, K., D. Quandt, K. Schubert, M. Rossol, M. Klingner, S. Jasinski-Bergner, R. Scholz, B. Seliger, M. Pierer, C. Baerwald, and U. Wagner. 2016. Latent Cytomegalovirus Infection in Rheumatoid Arthritis and Increased Frequencies of Cytolytic LIR-1+CD8+ T Cells. Arthritis Rheumatol. 68:337–346.

Rudolph, M. G., J. A. Speir, A. Brunmark, N. Mattsson, M. R. Jackson, P. A. Peterson, L. Teyton, and I. A. Wilson. 2001. The Crystal structures of Kbm1 and Kbm8 reveal that subtle changes in the peptide environment impact thermostability and alloreactivity. Immunity 14:231–242.

Schiefner, A., M. Fujio, D. Wu, C. H. Wong, and I. A. Wilson. 2009. Structural evaluation of potent NKT cell agonists: implications for design of novel stimulatory ligands. J. Mol. Biol. 394:71–82.

Tedla, N., H. An, L. Borges, U. Vollmer-Conna, K. Bryant, C. Geczy, and H. P. McNeil. 2011. Expression of activating and inhibitory leukocyte immunoglobulin-like receptors in rheumatoid synovium: correlations to disease activity. Tissue Antigens 77:305–316.

Truong, A. D., J. Ban, B. Park, Y. H. Hong, and H. S. Lillehoj. 2016. Characterization and functional analyses of a novel chicken CD8alpha variant X1 (CD8alpha1). J. Anim. Sci. 94:2737–2751.

Truong, A. D., Y. Hong, C. T. Hoang, J. Lee, and Y. H. Hong. 2017. Chicken IL-26 regulates immune responses through the JAK/STAT and NF-kappaB signaling pathways. Dev. Comp. Immunol. 73:10–20.

Truong, A. D., Y. Hong, J. Lee, K. Lee, H. T. T. Tran, H. V. Dang, V. K. Nguyen, H. S. Lillehoj, and Y. H. Hong. 2018a. Chicken novel leukocyte immunoglobulin-like receptor subfamilies B1 and B3 are transcriptional regulators of MHC class I genes and signaling pathways. Asian-Australas. J. anim. sci. doi 10.5713/ajas.18.0561.

Truong, A. D., Y. H. Hong, and H. S. Lillehoj. 2015. High-throughput sequencing reveals differing immune responses in the intestinal mucosa of two inbred lines afflicted with necrotic enteritis. Vet. Immunol. Immunopathol. 166:116–124.

Truong, A. D., Y. H. Hong, and H. S. Lillehoj. 2015b. RNA-seq profiles of immune related genes in the spleen of necrotic enteritis-afflicted chicken lines. Asian Australas. J. Anim. Sci 28:1496–1511.

Truong, A. D., B. Park, J. Ban, and Y. H. Hong. 2016. The novel chicken interleukin 26 protein is overexpressed in T cells and induces proinflammatory cytokines. Vet. Res. 47:65.

Truong, A. D., D. Rengaraj, Y. Hong, H. T. T. Tran, H. V. Dang, V. K. Nguyen, H. S. Lillehoj, and Y. H. Hong. 2018b. Leukocyte Immunoglobulin-like receptors A2 and A6 are expressed in Avian macrophages and modulate cytokine production by activating multiple signaling pathways. Int. J. Mol. Sci. 19. doi 10.3390/ijms19092710.

Uchtenhagen, H., E. T. Abualrous, E. Stahl, E. B. Allerbring, M. Sluijter, M. Zacharias, T. Sandalova, T. van Hall, S. Springer, P. A. Nygren, and A. Achour. 2013. Proline substitution independently enhances H-2D(b) complex stabilization and TCR recognition of melanoma-associated peptides. Eur. J. Immunol. 43:3051–3060.

Vilcek, J., and M. Feldmann. 2004. Historical review: Cytokines as therapeutics and targets of therapeutics. Trends Pharmacol. Sci. 25:201–209.

Vivier, E., and M. Daeron. 1997. Immunoreceptor tyrosine-based inhibition motifs. Immunol. Today 18:286–291.

Zhang, F., J. Zheng, X. Kang, M. Deng, Z. Lu, J. Kim, and C. Zhang. 2015a. Inhibitory leukocyte immunoglobulin-like receptors in cancer development. Sci. China Life Sci. 58:1216–1225.

Zhang, Z., H. Hatano, J. Shaw, M. Olde Nordkamp, G. Jiang, D. Li, and S. Kollnberger. 2015b. The Leukocyte immunoglobulin-like receptor family member LILRB5 binds to HLA-Class I heavy chains. PLoS One 10:e0129063.